High-performance velocity, frequency and time estimation using GNSS

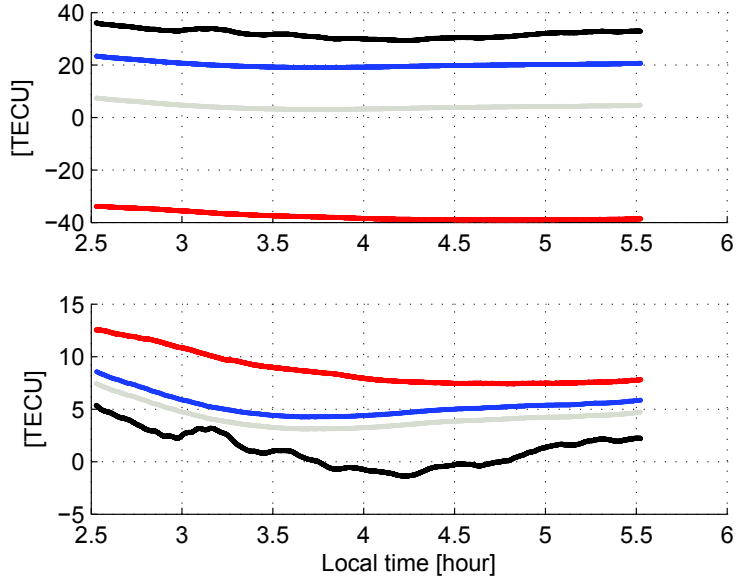

Figure 11.18: sTEC (upper plots) and sTEC zero-normalized (lower plots) measurements comparison, March 25^{th}, 2011, PRN 28. MAPGPS (gray), Ashtech (blue), CRS (black), NovAtel (red).

the coordinates of the Arecibo Observatory are 18.344 N, 66.753 W. Therefore the TEC estimate which on the grid is closest to Arecibo is the one comprised between 17.5 and 20 degrees in longitude and between 65 and 70 degrees in latitude. Using the data provided by JPL, it is possible to find a value of TEC every 2 hours.

Figure 11.19 and Figure 11.20 show the JPL vTEC estimate (black plots) for March 25^{th} and 27^{th}, respectively, compared with GNSS receivers measurements (Ashtec receiver, in blue).

In Figure 11.19 a comparison is shown with the vTEC from the Ashtech receiver and the JPL map.

JPL measurements do not present a bias with respect to the measure of the receivers, but they reveal a larger value during the higher ionosphere activities, while it is closer to zero during the minimum ionospheric activity. The time when the minimum is measured is about the same with the three receivers, while the JPL map indicates a different time for the maximum. This could likely be improved by using grid interpolation and by decreasing the JPL map update time interval.

Figure 11.20, which is for March 27^{th}, in comparison with Figure 11.19, which is

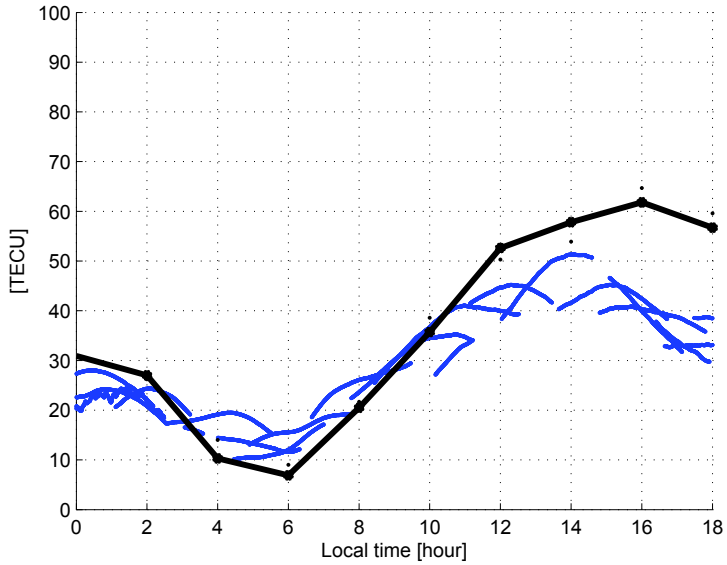

Figure 11.19: Comparison between JPL map (black) and Ashtech (blue) vTEC measurement, March 25^{th} 2011.

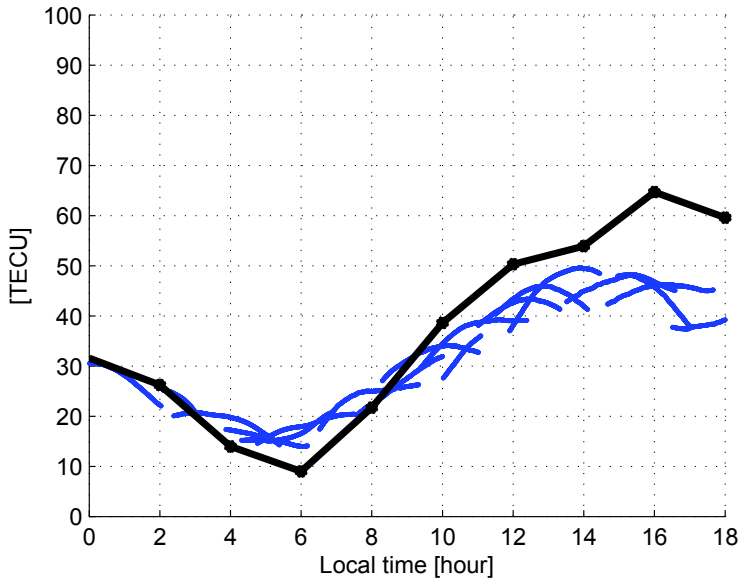

Figure 11.20: Comparison between JPL map (black) and Ashtech (blue) vTEC measurement, March 27^{th} 2011.

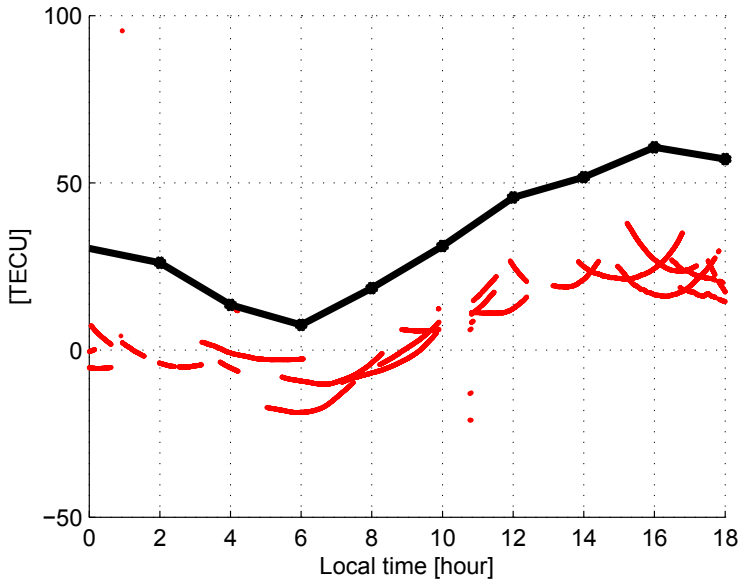

Figure 11.21: Comparison between JPL map (black) and Septentrio (red) vTEC measurement, March 26^{th} 2011.

related to March 25^{th}, shows how the relative error in between the Ashtech vTEC (blue) and the JPL estimate (black) does not change significantly for different days, which means that the bias component on the estimate is not changing significantly over time.

In Figure 11.21, a comparison is shown with the Septentrio receiver for March 26^{th}, and the result is comparable with the one obtained with the other receiver, even if the sign of the Septentrio bias is negative (effect which is clearly due to the receiver bias).

Some data from the ISR in Arecibo were also analyzed. The data provided by the observatory consist of electron density at specific altitudes. In particular, the heights scanned are from 90 to about 2350 km, at an interval in altitude of 1 km. The electron density profiles are provided approximatively every 30 minutes.

Figure 11.9 and Figure 11.11 show radar profiles measured on March 25^{th} 2011 and on March 27^{th} 2011, respectively. By integrating the profiles along the measured altitudes, vertical TEC measurements are obtained.

Some comparisons with the ISR data are shown in Figure 11.22 and in Figure 11.23, which are from March 25^{th} and March 27^{th}, respectively. From the comparison, a bias of about 12 TECU between the Ashtech (blue) and the ISR (red, continuous line) is present in the data. This seems to indicate that the radar is

calibrated to provide a minimum TEC measurement of zero TECU. In Figure 11.22 and Figure 11.23 another comparison is also shown, between the Ashtech measurements and the radar vTEC measurements shifted by +12.5 TECU (red, dashed) in order to verify the agreement level between the Ashtech and the ISR estimates. It can be noted that, apart differences that are mainly due to the OF accuracy, the maximum relative measurements disagreement is less than 5 TECU. The vTEC variations over time closely agree between the ISR and GPS receivers.

11.6 Final remarks on TEC measurements

Measurement comparisons have been done that demonstrate how, at the state of the art, dual-frequency GNSS TEC measurement are affected by errors, in particular, by large biases, mostly due to frequency-variant receiver biases. These TEC measurement errors impact on the time estimate depending on the geometry and cannot be neglected when high-accuracy is required on the time solution.
Application of the modified CNMP algorithm enables the reduction of noise and multipath on the pseudorange TEC measurements, including a good estimate of the remaining bias. Furthermore, the algorithm enables the definition of a bound on the accuracy of the bias estimate due to the presence of multipath. This is very important in order to define a confidence level, in particular when the measurement is performed in environments not benign in terms of multipath. For the data reported in this thesis, the multipath bound was found to be less than 1 TECU on the L1-GPS channel.
Concerning the other bias components, from the analysis of multiple data sources and methods it can be concluded that it is very difficult to separate the effects of the ionosphere and the biases of the GPS measurement system. Combining all the calibration and filtering methods used so far, the accuracy of the absolute TEC measurements is on the order of 10 TECU.
The hardware calibration used by CRS does not improve the knowledge of the absolute bias on the TEC measurement, even if it improves the performance in terms of relative bias between the satellites, mitigating the inter-frequency and inter-code receiver biases. This uncertainty has to be taken into account, in particular when high accuracy is required for absolute measurements, such as for time measurement.

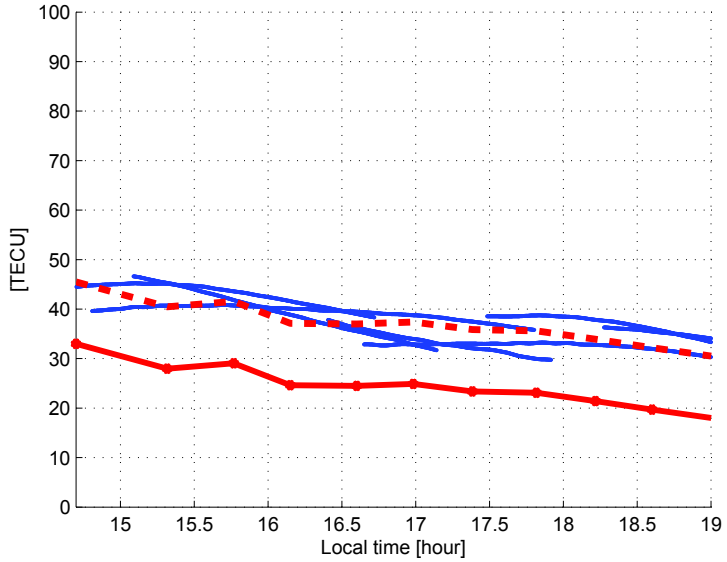

Figure 11.22: vTEC measurements, comparison between Ashtech receiver (blue), Arecibo ISR (red, solid line) and Arecibo ISR shifted by +12.5 TECU (red, dash line) for comparison purposes. March 25^{th} 2011.

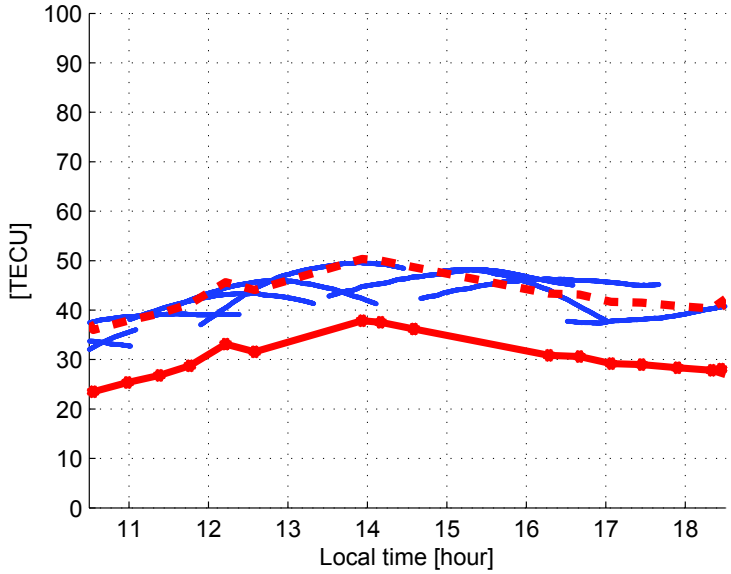

Figure 11.23: vTEC measurements, comparison between Ashtech receiver (blue), Arecibo ISR (red, solid line) and Arecibo ISR shifted by +12.5 TECU (red, dash line) for comparison purposes. March 27^{th} 2011.

In conclusion, it can be stated that an uncertainty on the order of 10 TECU on the TEC measurement is present in GNSS receivers, that causes uncertainty on the time measurement, in a measure that depends on the DOP (see Chapter 2). The next step, in order to improve the accuracy on the ionospheric delay estimate and therefore on the time estimate, includes a more rigorous receiver hardware, front-end and antenna calibration that takes into account the receiver bandwidth, correlator type and differential group delays for all the receivers involved in the TEC estimation process.

Conclusions

Conclusions and Future Activities

A new approach has been investigated to improve the GNSS precise velocity measurement, by means of a frequency-integrated solution.
The main issue of this activity is to correctly model the local oscillator, in order to improve the GNSS frequency measurement filtering it taking into account the model.
Then, since the precise velocity estimate is done by using the carrier phase measurement to enable mm/s level accuracy, a way to reduce the tracking jitter has been analyzed. The method considered makes use of a stand alone digital PLL implemented in a real-time software receiver. Novel adaptive DPLLs have been designed of different order (second and third), whose bandwidth is adapted in real-time according to the input signal. The goal is to use the smallest bandwidth that can still correctly track the current input dynamics, and in order to do that a cost function is minimized.
Regarding this work on precise velocity and frequency, much work remains on the to-do-list for the future. Since the frequency estimate is intended to improve the frequency estimate, the scenario of interest involves dynamic user. Therefore the future work includes improving the frequency estimate by including dynamic models of the oscillator (Rubidium oscillators in particular). Then, the frequency estimate has to be integrated with the improved carrier phase measurement performed by the adaptive PLL. Also, more tests with real data have to be done in order to optimize the control logic of the PLL.
In order to improve high accuracy time estimate, analysis have been done on the existing TEC measurement method. After the analysis of the measurement campaign, a modified CNMP method was applied to mitigate noise and multipath effects. Future work has to be done, including the development of methods to mitigate the TEC biases, in particular, the biases due to the receiver hardware. An accurate design or calibration of the hardware and the use of a calibrate

network of receivers could be a solution to mitigate the problem of the unknown residual biases, enabling highly accurate time measurements.

Appendixes and Bibliography

Appendix A

Derivation of the loop filter coefficients given the PLL ENB

The method used in this thesis to find the coefficients of the loop filter in a first and in a second order PLL, as a function of EBN, is taken from [67] and it is recalled in this appendix.

A.1 First order loop

In a first order PLL the loop filter is constituted simply by a constant parameter, i.e. :

$$F(z) = \gamma \tag{A.1}$$

and it is

$$B_L T \simeq \frac{A}{4} \tag{A.2}$$

where $A = \gamma\beta$ Therefore, the filter parameter can be expressed as:

$$\gamma = \frac{4B_L T}{\beta} \tag{A.3}$$

A.2 Second order loop

In case of second order loop, the loop filter can be expressed as:

$$F(z) = \frac{az - b}{z - 1} \tag{A.4}$$

A relationship is needed to find the loop coefficients a, b as functions of the ENB. In the following, the relationship is derived, by introducing some approximation, as in [67].

A.3 Approximation 1

The link with the analog case can be findable through some algebraical artifices. Regarding in particular the denominator, it can be defined the function

$$R(z) = \frac{1}{(z-1)^2 + \beta \cdot (az - b)}. \tag{A.5}$$

It is also

$$R(z) = \left(\frac{z^{-1}}{M \sin \alpha}\right) \sum_{i=0}^{\infty} M^i \sin(k\alpha)\, z^{-i} \tag{A.6}$$

where

$$\begin{aligned} M &= e^{-\zeta \omega_n T} \\ \alpha &= \omega_n T \cdot \sqrt{1-\zeta^2} \end{aligned}$$

For $k > 0$ it is

$$R[k] = \frac{1}{M \sin \alpha} M^{k-1} \sin[(k-1)\alpha] \tag{A.7}$$

Working in the Laplace domain, if

$$(p,\, p*) \tag{A.8}$$

is the complex conjugate couple of poles for $R(z)$, and

$$p = \sigma_0 + j\omega_0 \tag{A.9}$$

it is possible to find a relation between two analog parameters.

The natural frequency is

$$\omega_n = |p| \tag{A.10}$$

and the damping factor

$$\zeta = -\frac{\sigma_0}{|p|}. \tag{A.11}$$

Inverting these formulas it can be found that

$$\begin{aligned} \sigma_0 = &\quad \zeta\omega_n \\ \omega_0 = &\quad \omega_n\sqrt{1-\zeta^2} \end{aligned}$$

Using these parameters it can be written:

$$R(s) = \frac{1}{s^2 - 2\zeta\omega_n \cdot s + \omega_n^2}. \tag{A.12}$$

The parallelism between the digital and the analog worlds allows in this case to easly project a digital loop. In fact, fixing some analog entities it is possible to compute the loop coefficients. For the second order loop, as it has been showed, two parameters

$$(a,\, b) \tag{A.13}$$

are involved.

It has been discussed how the noise equivalent bandwidth is determinant for the PLL performance. So one of the characteristics that would be appropriate to fix is exactly this parameter. The other one could be the damping factor.

It can be found that

$$\begin{aligned} a \simeq &\quad \tfrac{1}{\beta} \cdot 2\left(1 - e^{-\zeta\omega_n T}\cos\left(\omega_n T \cdot \sqrt{1-\zeta^2}\right)\right) \\ b \simeq &\quad \tfrac{1}{\beta} \cdot \left(1 - e^{-2\zeta\omega_n T}\right) \end{aligned}$$

Considering one of the two equations above and the relationship that links the noise equivalent bandwidth to the loop coefficients, that is

$$B_L T = \frac{2(a-b) + \beta b(a+b)}{2b\left[4 - \beta(a+b)\right]}. \tag{A.14}$$

it is possible to determine the a, b values as functions of B_L, ζ, ω_n and T, T is considered fixed by the user and in this case is fixed at $T = 1$ ms (like most GPS applications). Generally it is

$$\zeta = \sqrt{2} \tag{A.15}$$

Considering the equations system above, the bandwidth can be expressed as

$$B_L \simeq \omega_n \cdot \frac{1+4\zeta^2}{8\zeta} \tag{A.16}$$

so the natural frequency becomes known as a (B_L, ζ)

function

$$\omega_n = \frac{8\zeta B_L}{1+4\zeta^2} \tag{A.17}$$

and the loop coefficients can easly be calculated using the previous formulas:

$$a \simeq \frac{1}{\beta} \cdot 2\left(1 - e^{-\zeta\omega_n T}\cos\left(\omega_n T \cdot \sqrt{1-\zeta^2}\right)\right) \tag{A.18}$$

$$b \simeq \frac{1}{\beta} \cdot \left(1 - e^{-2\zeta\omega_n T}\right) \tag{A.19}$$

A.3.1 Approximation 2

In this thesis, another approximation for the loop coefficients is used, that makes use of the approximation described in A.3. This method uses a transform similar to the bilinear one, that implies

$$z = 1 + sT \tag{A.20}$$

Equation A.12 can be written as:

$$R(s) = \frac{1}{\left((1+sT)-1\right)^2 + \beta \cdot \left(a\left(1+sT\right) - b\right)}. \tag{A.21}$$

Then, making a comparison with the analog case (Equation A.18), as done in the A.3, the parameters a, b can be found, that are used in this thesis, as a function of the a parameter δ (see Equation A.24), proportional to the ENB B_L:

$$a = \frac{1}{\beta} \cdot 4\zeta^2 \frac{\delta}{1+\delta} \tag{A.22}$$

$$b = \frac{1}{\beta} \cdot 4\zeta^2 \frac{\delta}{(1+\delta)^2} \tag{A.23}$$

where it has been defined

$$\delta = \frac{4B_L T}{1 + 4\zeta^2 + 8\zeta^2 B_L T}. \tag{A.24}$$

A.4 Third order loop

It is not trivial to find the coefficients of a second order loop given a desired bandwidth, considering that the stability condition needs to be satisfied. The problem becomes even more complicated when three parameters are required, as in the case of a third order PLL. In this thesis, the method proposed in [68] is used.
According to [68]

The zero coincidence condition is desired, thus

$$z_2 = z_1 \tag{A.25}$$

Having real and coincident zeros do not preclude any possibilities, since every bandwidth can be obtained in this way. With the hypothesis that have been done, the bandwidth results to be

$$B_{eq} = \frac{g}{2T} \frac{g z_1^5 + (3g-5) z_1^4 + 3g z_1^3 + (g-1) z_1^2 + 5 z_1 + 1}{-g^2 z_1^5 - 3g^2 z_1^4 + (7g - 3g^2) z_1^3 + (7g - g^2) z_1^2 + (8+g) z_1 + (-8+g)} \tag{A.26}$$

Another approximation is required. The limit values for z_1 that allows to obtain stable loops is

$$1 - 2g < z_1 < 1 \tag{A.27}$$

By choosing the middle value

$$z_1 = \frac{1 + (1-2g)}{2} \tag{A.28}$$

so that

$$g = 1 - z_1 \tag{A.29}$$

it becomes

$$\lim_{z_1 \longrightarrow 1} B_L = \frac{5}{4T} (1 - z_1) \tag{A.30}$$

So, fixing the desired value of B_L, it is

$$z_1 = 1 - \frac{4}{5} \cdot B_L \cdot T \tag{A.31}$$

The relationship between this parameter and the loop coefficient results to be simply:

$$\begin{cases} a = & 1 \\ b = & -(z_1 + z_2) \\ c = & z_1 \cdot z_2 \end{cases} \tag{A.32}$$

Because of the approximation, the effective noise equivalent bandwidth realized by the loop is not exactly as desired, but it represents a good approximation (approximation error within the 2 percent).

After several simulation, by empiric analysis it has been noted that the more g is close to the parameter $B_L \cdot T$, the more the approximation is valid.

Setting

$$z_1 = 1 - \frac{h-1}{h} \cdot B_L \cdot T \tag{A.33}$$

with $h = 30$ the approximate B_L results to be very close to the desired value.

Appendix B

Tracking Steady State Error as a function of the input dynamics and of the PLL order

B.1 First order loop

The loop error results to be

$$\begin{aligned} \rho(z) &= \frac{z}{(z-1)+\beta \cdot F(z)} \cdot \Delta_\phi(z) \\ &= \frac{z}{z+(A-1)} \cdot \Delta_\phi(z) \end{aligned}$$

calling

$$A = a \cdot \beta \tag{B.1}$$

In order to see the loop behaviour, it is useful to pass in the time domain ([66]). It is:

$$\begin{aligned} \rho(z) \cdot [z+(A-1)] &= z \cdot (z) \\ z \cdot \rho(z) + (A-1) \cdot \rho(z) &= z \cdot \Delta_\phi(z) \\ \rho[k+1] - (A-1) \cdot \rho[k] &= \Delta_\phi[k+1] \\ \rho[k+1] &= (1-A) \cdot \rho[k] + \Delta_\phi[k+1] \end{aligned}$$

That means (substituting the variable k with $k-1$):

$$\rho[k] = (1-A) \cdot \rho[k-1] + \Delta_\phi[k] \tag{B.2}$$

With this expression it is easy to understand if, given a signal with a specified phase trend, the loop error will converge towards zero.
Notice that in this analysis an ideal case is studied and the noise effect is neglected.

B.1.1 First order loop, constant input phase

If the input is a step phase in the time,

$$\phi[k] = A_0 \cdot u[k] \tag{B.3}$$

the phase variation to be followed is

$$\begin{aligned} \Delta_\phi[k] &= \phi[k] - \phi[k-1] \\ &= A_0 \cdot u[k] - A_0 \cdot u[k-1] \\ &= A_0 \cdot \delta[k] \end{aligned}$$

So it is

$$\begin{aligned} \rho[k] &= (1-A) \cdot \rho[k-1] + \Delta_\phi[k] \\ &= (1-A) \cdot \rho[k-1] + A_0 \cdot \delta[k] \end{aligned}$$

The error trend is therefore computable simply iterating:

If $k = 0$:

$$\begin{aligned} \rho[0] &= A_0 \cdot \delta[0] \\ &= A_0 \end{aligned}$$

if $k = 1$:

$$\begin{aligned} \rho[1] &= (1-A) \cdot \rho[0] + A_0 \cdot \delta[1] \\ &= (1-A) \cdot A_0 + 0 \\ &= A_0 \cdot (1-A) \end{aligned}$$

if $k = 2$

$$\begin{aligned}\rho[2] &= (1-A)\cdot\rho[1] \\ &= A_0\cdot(1-A)^2\end{aligned}$$

if $k=3$

$$\begin{aligned}\rho[3] &= (1-A)\cdot\rho[1] \\ &= A_0\cdot(1-A)^3\end{aligned}$$

:

if $k=n$

$$\rho[n] = A_0\cdot(1-A)^n$$

that means that the error follows a geometric law. Since

the error decrease towards zero only if

$$|1-A|<1. \tag{B.4}$$

where $A=\gamma\beta$.

B.1.2 First order loop, first order input phase

If the input phase varies with linear law, i.e.

$$\phi[k] = A_1\cdot k\cdot u[k] \tag{B.5}$$

the variation is

$$\Delta_\phi[k] = A_1\cdot\delta[k]. \tag{B.6}$$

Thinking about the signal, the input derivative represents the input frequency, since the frequency is the phase derivative in the time. Proceeding like in the previous case, it can be computed

$$\begin{aligned}\rho[k] &= (1-A)\cdot\rho[k-1]+\Delta_\phi[k] \\ &= (1-A)\cdot\rho[k-1]+A_1\cdot\delta[k]\end{aligned}$$

If $k = 0$:

$$\begin{aligned} \rho[0] &= A_1 \cdot \delta[0] \\ &= A_1 \end{aligned}$$

if $k = 1$:

$$\begin{aligned} \rho[1] &= (1-A) \cdot \rho[0] + A_1 \cdot \delta[1] \\ &= (1-A) \cdot A_1 + A_1 \\ &= A_1 \cdot (2-A) \end{aligned}$$

if $k = 2$:

$$\begin{aligned} \rho[2] &= (1-A) \cdot \rho[1] + A_1 \\ &= (1-A) \cdot [(1-A) \cdot A_1 + A_1] + A_1 \\ &= (1-A)^2 \cdot A_1 + (1-A) \cdot A_1 + A_1 \end{aligned}$$

:

if $k = n$

$$\rho[n] = (1-A)^n \cdot A_1 + (1-A)^{n-1} \cdot A_1 + ... + (1-A) \cdot A_1 + A_1 \tag{B.7}$$

that can be written using the geometrical series

$$\sum_{i=0}^{n-1} x^i = \frac{1-x^n}{1-x} \tag{B.8}$$

$$\begin{aligned} \rho[n] &= A_1 \sum_{i=0}^{n} (1-A)^n \\ &= A_1 \frac{1-(1-A)^{n+1}}{1-(1-A)} \end{aligned}$$

To solve the limit

$$\lim_{k \to \infty} \rho[k] \tag{B.9}$$

the final value theorem that is valid for the Z-transform can be used:

$$\begin{aligned}\lim_{k\to\infty}\rho[k] &= \lim_{z\to 1}\{\rho(z)\cdot(z-1)\}\\ &= \lim_{z\to 1}\left\{\frac{z}{z+(A-1)}\cdot\Delta_\phi(z)\cdot(z-1)\right\}\\ &= \lim_{z\to 1}\left\{\frac{z\cdot(z-1)}{z+(A-1)}\cdot\Delta_\phi(z)\right\}\end{aligned}$$

It is

$$\begin{aligned}\Delta_\phi(z) &= \mathcal{Z}\{\Delta_\phi[k]\}\\ &= \mathcal{Z}\{\phi[k]-\phi[k-1]\}\\ &= \left(1-z^{-1}\right)\mathcal{Z}\{\phi[k]\}\\ &= \left(1-z^{-1}\right)\mathcal{Z}\{A_1\cdot k\cdot u[k]\}\\ &= A_1\left(1-z^{-1}\right)\left(-\frac{\delta}{\delta z}\left(\frac{1}{1-z^{-1}}\right)\right)\\ &= A_1\left(\frac{z-1}{z}\right)\frac{1}{(z-1)^2}\\ &= A_1\frac{1}{z(z-1)}\end{aligned}$$

$$\begin{aligned}\lim_{k\to\infty}\rho[k] &= \lim_{z\to 1}\left\{\frac{z\cdot(z-1)}{z+(A-1)}\cdot A_1\frac{1}{z(z-1)}\right\}\\ &= \frac{A_1}{A}\neq 0\end{aligned}$$

This result means that a first order loop cannot track a phase that varies linearly, since the error does not converges towards zero. A constant SSE (Steady State Error) is present, directly proportional to the slope of the linear input and inversely proportional to the bandwidth (since the parameter A is directly proportional to B_L).

B.1.3 First order loop, second order input phase

In the case of linear input frequency, the phase varies following a quadratic law and the a first order PLL cannot track it. In this case the phase error results to be a function of the time k, therefore it does not converge, but it increases in the time.

B.2 Second order loop

Like done for the first order loop, the error can be computed as

$$\begin{aligned}\rho(z) &= \frac{z}{(z-1)+\beta\cdot F(z)}\cdot\Delta_\phi(z)\\ &= \frac{z(z-1)}{(z-1)^2+\beta\cdot(az-b)}\cdot\Delta_\phi(z)\end{aligned}$$

In the time domain.

$$\begin{aligned}\rho(z)\cdot\left[(z-1)^2+\beta\cdot(az-b)\right] &= z(z-1)\cdot\Delta_\phi(z)\\ z^2\cdot\rho(z)+(a\beta-2)\,z\cdot\rho(z)+(1-b\beta)\cdot\rho(z) &= z^2\cdot\Delta_\phi(z)-z\cdot\Delta_\phi(z)\\ \rho[k+2]+(a\beta-2)\,\rho[k+1]+(1-b\beta)\cdot\rho[k] &= \Delta_\phi[k+2]-\Delta_\phi[k+1]\end{aligned}$$

So:

$$\rho[k+2]=(2-a\beta)\,\rho[k+1]+(b\beta-1)\cdot\rho[k]+\Delta_\phi[k+2]-\Delta_\phi[k+1] \quad \text{(B.10)}$$

Sobstituting the variable k with $k-2$:

$$\rho[k]=(2-a\beta)\,\rho[k-1]+(b\beta-1)\cdot\rho[k-2]+\Delta_\phi[k]-\Delta_\phi[k-1] \quad \text{(B.11)}$$

B.2.1 Second order loop, first order input phase

Like said for the order one PLL, this input is

$$\phi[k]=A_1\cdot k\cdot u[k] \quad \text{(B.12)}$$

and its variation

$$\Delta_\phi[k]=A_1\cdot\delta[k]. \quad \text{(B.13)}$$

$$\begin{aligned}\rho[k] &= (2-a\beta)\,\rho[k-1]+(b\beta-1)\cdot\rho[k-2]+\Delta_\phi[k]-\Delta_\phi[k-1]\\ &= (2-a\beta)\,\rho[k-1]+(b\beta-1)\cdot\rho[k-2]+A_1\cdot\delta[k]-A_1\cdot\delta[k-1]\end{aligned}$$

If $k = 0$:

$$\begin{aligned}\rho[0] &= A_1 \cdot \delta[0] \\ &= A_1\end{aligned}$$

if $k = 1$:

$$\begin{aligned}\rho[2] &= (2 - a\beta)\,\rho[0] + A_1 \cdot \delta[1] - A_1 \cdot \delta[0] \\ &= (2 - a\beta)\,A_1 - A_1 \cdot 1 \\ &= A_1\{(2 - a\beta) - 1\}\end{aligned}$$

if $k = 2$:

$$\begin{aligned}\rho[2] &= (2 - a\beta)\,\rho[1] + (b\beta - 1) \cdot \rho[0] + A_1 \cdot \delta[2] - A_1 \cdot \delta[1] \\ &= (2 - a\beta) \cdot ((2 - a\beta)\,A_1 - A_1) + (b\beta - 1) \cdot A_1 \\ &= A_1\left\{(2 - a\beta)^2 - (2 - a\beta) + (b\beta - 1)\right\}\end{aligned}$$

if $k = 3$:

$$\begin{aligned}\rho[3] &= (2 - a\beta)\,\rho[2] + (b\beta - 1) \cdot \rho[1] \\ &= A_1\left\{(2 - a\beta)^3 - (2 - a\beta)^2 + 2\,(b\beta - 1)\,(2 - a\beta) - (b\beta - 1)\right\}\end{aligned}$$

if $k = 4$:

$$\begin{aligned}\rho[4] &= (2 - a\beta)\,\rho[3] + (b\beta - 1) \cdot \rho[2] \\ &= A_1\left\{(2 - a\beta)^4 - (2 - a\beta)^3 + 3\,(b\beta - 1)\,(2 - a\beta)^2 - 2\,(b\beta - 1)\,(2 - a\beta) + (b\beta - 1)^2\right\}\end{aligned}$$

This approach does not allow to easy find out if the error converges towards zero.
In this case in convenient to consider that

$$\begin{aligned}\rho(z) &= \frac{z\,(z-1)}{(z-1)^2 + \beta \cdot (az - b)} \cdot \Delta_\phi(z) \\ &= R(z) \cdot z\,(z-1) \cdot \Delta_\phi(z) \\ &= z\,(z-1) \cdot \Delta_\phi(z) \left(\frac{z^{-1}}{M \sin\alpha}\right) \sum_{i=0}^{\infty} M^i \sin(k\alpha)\, z^{-i} \\ &= (z-1) \cdot \frac{A_1}{z-1} \left(\frac{1}{M \sin\alpha}\right) \sum_{i=0}^{\infty} M^i \sin(k\alpha)\, z^{-i} \\ &= A_1 \left(\frac{1}{M \sin\alpha}\right) \sum_{i=0}^{\infty} M^i \sin(k\alpha)\, z^{-i}\end{aligned}$$

That in the time domain is:

$$\rho[k] = A_1 \frac{1}{M \sin\alpha} M^k \sin[k\alpha]. \tag{B.14}$$

In this way it is easy calculating the error:

if $k = 0$:

$$\begin{aligned} \rho[0] &= A_1 \frac{1}{M \sin\alpha} M^2 \sin(2\alpha) \\ &= 0 \end{aligned}$$

if $k = 1$:

$$\begin{aligned} \rho[1] &= A_1 \frac{1}{M \sin\alpha} M \sin\alpha \\ &= A_1 \end{aligned}$$

if $k = 2$:

$$\begin{aligned} \rho[2] &= A_1 \frac{1}{M \sin\alpha} M^2 \sin(2\alpha) \\ &= \frac{A_1}{\sin\alpha} \cdot M \sin(2\alpha) \end{aligned}$$

...

if $k = n$:

$$\rho[n] = \frac{A_1}{\sin\alpha} \cdot M^{n-1} \sin(n \cdot \alpha) \tag{B.15}$$

$$\begin{aligned} \lim_{n \longmapsto \infty} \rho[n] &= \lim_{n \longmapsto \infty} A_1 \frac{\sin(n \cdot \alpha)}{\sin\alpha} \cdot M^{n-1} \\ &= 0 \text{ , if } M < 1. \end{aligned}$$

If $M < 1$

the error converge towards zero. The limit decays faster if M

is smaller. In this trend the important parameter is the damping factor ζ

, since it is

$$M = e^{-\zeta \omega_n T}. \tag{B.16}$$

B.2.2 Second order loop, second order input phase

A phase that changes with a parabolic law can be expressed as

$$\phi[k] = A_2 \cdot k^2 \cdot u[k] \tag{B.17}$$

the variation is, in the time domain

$$\Delta_\phi[k] = 2 \cdot A_2 \cdot k \cdot u[k] \tag{B.18}$$

and in the z-transform domain

$$\Delta_\phi(z) = A_2 \cdot \frac{z+1}{(z+1)^2} \tag{B.19}$$

Applying the final value theorem it can be found the error convergence towards infinity:

$$\begin{aligned}
\lim_{k\to\infty} \rho[k] &= \lim_{z\to 1} \{\rho(z) \cdot (z-1)\} \\
&= \lim_{z\to 1} \left\{ \frac{z(z-1)}{(z-1)^2 + \beta \cdot (az-b)} \cdot \Delta_\phi(z) \cdot (z-1) \right\} \\
&= \lim_{z\to 1} \left\{ \frac{z(z-1)}{(z-1)^2 + \beta \cdot (az-b)} \cdot A_2 \cdot \frac{z+1}{(z+1)^2} \cdot (z-1) \right\} \\
&= \lim_{z\to 1} \left\{ \frac{z}{(z-1)^2 + \beta \cdot (az-b)} \cdot A_2 \cdot (z+1) \right\} \\
&= \frac{2A_2}{\beta(a-b)} \neq 0
\end{aligned}$$

This results means that a second order loop is not able to vanish the estimation error if the input phase increase quadratically. As well as a linear phase cannot be tracked with zero SSE by a first order PLL, while a second order PLL can do it, a second order loop cannot track a quadratic input phase but a third order can do it. This is why in this thesis also a third order loop is studied.

Bibliography

[1] F. van Graas L. Mart. Bias detection and its confidence assessment in global positioning system signals. *2004 IEEE Aerospace Conference Proceedings*, 2004.

[2] A. Soloviev F. van Graas. Precise velocity estimation using a stand-alone gps receiver. *NAVIGATION, Vol. 51, No. 4, Winter 2004-2005, pp. 283-292*, 2004.

[3] C. J. Hegarty E. D. Kaplan. *Understanding GPS, principles and applications, Second Edition*. Artech House, 2006.

[4] NAP. Website: http://www.nap.edu.

[5] Official U.S. Government information about the Global Positioning System (GPS) and related topics. Website: http://www.gps.gov/.

[6] E. D. Kaplan. *Understanding GPS, principles and applications, First Edition*. Artech House, 1996.

[7] NewsMilitary online. Website: http://newsmilitary.com/.

[8] IEEE. Website: http://www.ieee-uffc.org/frequency_control/teaching.asp?vig=vigcomp.

[9] NASA. Website: http://www.nasa.gov.

[10] South African Journal of Science. Website: http://www.scielo.org.za/.

[11]

[12] Arecibo Observatory. Website: http://www.naic.edu.

[13] International Radio Occultation Working Group. Website: http://www.irowg.org.

[14] O. L. Sentman. Navy navigation satellite (transit). *IEEE AES Magazine, July 1987*, 1987.

[15] W. H. Jones. Navstar global positioning system: progress report. *IEEE AES Magazine, March 1987*, 1987.

[16] C. E. Pelc. Gps program status. *IEEE AES Magazine, May 1987*, 1987.

[17] M. J. Ellett. Civil access to navstar gps. 1987.

[18] B. W. Parkinson and P. K. Enge. *Global Positioning System: Theory and applications*. American Institute of Aeronautics and Astronautics, Inc., 2000.

[19] P. Daly S. A. Dale. The soviet union's glonass navigation satellites. *IEEE AES Magazine, May 1987*, 1987.

[20] J. Leva. An alternative closed-form solution to the gps pseudo-range equations. *IEEE Trans Aerospace and Electronic Systems*, v. 32, 1996.

[21] P. Misra and P. K. Enge. *Global Positioning System - Signals, Measurements, and Performance*. American Institute of Aeronautics and Astronautics, Inc., 2000.

[22] W. Zhuang. Performance analysis of gps carrier phase observable. *IEEE TRANSACTIONS ON AEROSPACE AND ELECTRONIC SYSTEMS VOL. 32, NO. 2 APRIL 1996*, 1996.

[23] C. Altmayer. Enhancing the integrity of integrated gps/ins systems by cycle slip detection and correction. *Proceedings of the IEEE Intelligent Vehicles Symposium 2000, Dearborn (MI), USA October 3-5, 2000*, 2000.

[24] M. Nicola M. Fantino, A. Molino. N-gene gnss receiver: Benefits of software radio in navigation. *Congresso ENC GNSS 2009, 3-6 maggio 2009, Napoli, Italia*, 2009.

[25] N. Bertlsen P. Rinder S. H. Jelsen K. Borre, D. M. Akos. *A Software-Defined GPS and Galileo Receiver, A Single-Frequency Approach*. Birkhauser Boston, 2007.

[26] P.E. Talley Jr. A. S. Liu. Cesium beam phase and frequency measurements using gps time transfer techniques. 1988.

[27] D. Borio; C. O.Driscoll; J. Fortuny. Gnss jammers: Effects and countermeasures. *6th ESA Workshop on Satellite Navigation Technologies and European Workshop on GNSS Signals and Signal Processing, NAVITEC*, vol., no., pp.1-7, 5-7 Dec. 2012, 2012.

[28] B. Motella; M. Pini; M. Fantino; P. Mulassano; M. Nicola; J. Fortuny-Guasch; M. Wildemeersch; D. Symeonidis. Performance assessment of low cost gps receivers under civilian spoofing attacks. *Satellite Navigation Technologies and European Workshop on GNSS Signals and Signal Processing (NAVITEC), 2010 5th ESA Workshop on , vol., no., pp.1-8, 8-10 Dec. 2010*, 2010.

[29] R. B. Langley. Dilution of precision. *GPS World, May 1999*, 1999.

[30] J. Zhu. Calculation of geometric dilution of precision. *IEEE Transactions on Aerospace and Electronic Systems, July 1992*, 28, Issue: 3, Page(s): 893 - 895, 1992.

[31] C.W. Park J. How, N. Pohlman. Gps estimation algorithms for precise velocity, slip and race-track position measurements. 2002.

[32] *GNSS Aided Navigation and Tracking, Inertially augmented or autonomous.*

[33] W. Pelgrum F. van Graas, S. Craig. Laboratory and flight test analysis of rubidium frequency reference performance. 2011.

[34] Shoaf J. H. Halford D. Allan, D. W. *Statistics of Time and Frequency Data Analysis.* U. S. Department of Commerce, Frederick B. Dent, Secretary, and the National Bureau of Standards, Richard W. Roberts, Director, 1974.

[35] J. Rutman. Characterization of dhase and freauencv instabilities in precision frequency sources; fifteen years 6f prdgress. *proc.IEEE, vol. 66, pp. 1048-1174*, 1978.

[36] F. L. Walls J. Rutman. Characterization of frequency stability in precision frequency sources. *Proceedings of The IEEE - PIEEE , vol. 79, no. 7, pp. 952-960*, 1991.

[37] D. W. Allan. Statistics of atomic frequency standards. *Proceedings of the IEEE, Volume: 54 , Issue: 2, Page(s): 221 - 230*, 1966.

[38] J. Moses. Navstar global positioning system oscillator requirements for the gps manpack.

[39] L. A. Mallette T. A. McClelland J. Hardy N. D. Bhaskar, J. White. A historical review of atomic frequency standards used in space systems. *1996 IEEE Internetional Frequency Control Symposium*, 1996.

[40] *Satellite Communications and Navigation Systems.*

[41] X. Stehlin P. Rochat, B. Leuenberger. A new synchronized ultra miniature rubidium oscillator. *2002 IEEE lnternational Frequency Control Symposium and PDA Exhibition*, 2001.

[42] B. Guinot C. Audoin. *The measurement of Time. Time, frequency and the atomic clock.* Cambridge University Press, 2001.

[43] S. J. Lee M. Y. Shin, C. Park. Atomic clock error modeling for gnss software platform. 2008.

[44] P. Y. C. Hwang R. G. Brown. *Introduction to random signals and applied Kalman filtering, third edition.* 1997.

[45] NOAA NGDC. Website: http://www.ngdc.noaa.gov/geomagmodels/IGRFWMM.jsp.

[46] Pervan B. Chan F. C. Stochastic modeling of gps receiver clocks for improved positioning and fault detection performance. *Proceedings of the 22nd International Technical Meeting of The Satellite Division of the Institute of Navigation (ION GNSS 2009), Savannah, GA, September 2009, pp. 1652-1665*, 2009.

[47] Pervan B. Chan F.C., Joerger M. High integrity stochastic modeling of gps receiver clock for improved positioning and fault detection performance. *Proceedings of IEEE/ION PLANS 2010, Indian Wells, CA, May 2010, pp. 1245-1257*, 2010.

[48] Brown R. G. Dierendonck A. J., McGraw J. B. Relationship between allan variances and kalman filter parameters. *Proceedings of the 16th Precise Time and Time Interval Systems and Applications Meeting, 1984, pp. 273-293*, 1984.

[49] D. Slomovitz L. Trigo. Rubidium atomic clock with drift compensation. *2010 Conference on Precision Electromagnetic Measurements, June 13-18, 2010, Daejeon Convention Center, Daejeon, Korea*, 2010.

[50] R. E. Updegraf. Precise time and frequency control using the navstar gps and a disciplined rubidium oscillator.

[51] P. Jarlemark K. Jaldehag, C. Rieck. A gps carrier-phase aided clock transport for the calibration of a regional distributed time scale. 2009.

[52] Mr Clive Green Dr Cosmo Little. Gps disciplined rubidium oscillator. 1995.

[53] Z. Zhang. Impact of rubidium clock aiding on gps augmented vehicular navigation, 2010.

[54] L. Henrikson A. J. Bryson. Estimation using sampled data containing sequentially correlated noise. Journal of Spacecraft and Rockets, 5, 662-665.

[55] B. Pervan M. Joerger. Autonomous ground vehicle navigation using integrated gps and laser-scanner measurements. *IEEE*, 2006.

[56] B. Pervan M. Joerger. Range-domain integration of gps and laser scanner measurement. *ION GNSS 19th International Technical Meeting of the Satellite Division, 26-29 September 2006, Fort Worth, TX*, 2006.

[57] J. L. Farrell. Carrier phase coherence as a sequential correlation issue. *IEEE 2006*, 2006.

[58] C. Rizos K. Wang, Y. Li. Practical approaches to kalman filtering with time-correlated measurement errors. *IEEE TRANSACTIONS ON AEROSPACE AND ELECTRONIC SYSTEMS VOL. 48, NO. 2 APRIL 2012*, 2012.

[59] B. Christophe J. P. Chauveau, J. Lacroix. Time correlation of gps carrier phase measurements.

[60] G. Lachapelle M. E. Cannon M. G. Petovello, K. O.Keefe. Consideration of time correlated errors in a kalman filter applicable to gnss. *Springer Geodesy*, 2008.

[61] F.M. Gardner. *PhaseLock Techniques*. Wiley, 1964.

[62] D. B. Talbot. *Frequency Acquisition Techniques for Phase Locked Loops*. Wiley, 2012.

[63] R. E. Best. *Phase-locked loops: theory, design, and applications*. McGraw-Hill, 1993.

[64] U. L. Rohde. *Digital PLL frequency synthesizers: theory and design*. Prentice-Hall, 1983.

[65] M. A. Al-Qutayri S. R. Al-Araji, Z. M. Hussain. *Digital Phase Lock Loops: Architectures and Applications*. Springer, 2006.

[66] V.F. Kroupa. *Theory and Application of the Z-Transform Method*. Wiley, 2004.

[67] M. Visintin. Master in navigation, slides for the course carrier phase positioning - augmentations and integrity, 2010.

[68] M. Pent F. Dovis M. Falletti-F. Sellone G. Povero M. Visintin, M. Mondin. End-to-end study of gmsk modulation, esoc contract final report.

[69] M. Fantino G. Garbo M. Rao, L. Lo Presti. A software receiver phase lock loop analysis and design to implement adaptive phase tracking using a finite impulse response loop filter.

[70] T. H. Kwon Y. S. Choi, H. H Choi. An adaptive bandwidth phase locked loop with locking status indicator. *Div. of Electronic, Computer and Telecommunication Eng., Pukyong National University, Busan. 559-1. Korea, KORUS 2005*, 2005.

[71] E. Holland S. Rao G. Bishop, A. Mazzella. Algorithms that use the ionosphere to control gps errors.

[72] F.-R. Chang W.-L. Mao, H.-W. Tsao. Intelligent gps receiver for robust carrier phase tracking in kinematic environments. *IEE Proc.-Radar Sonar Navig., Vol. 151, No. 3, June 2004*, 2004.

[73] F. Legrand. Modele de boucle de poursuite de signaux a spectre etale et methode de amelioration de la precision des mesures brutes, 2002.

[74] J. L. Issler-L. Lestarquit C. Mehlen F. Legrand, C. Macabiau. Improvement of pseudoranges measurements accuracy by using fast adaptive bandwidth lock loops. *Proceedings of the 13th International Technical Meeting of the Satellite Division of the Institute of Navigation, Salt Lake City - 2000*, 2000.

[75] J.G. Garcia P.A. Roncagliolo. High dynamics and false lock resistant gnss carrier tracking loops. *International Technical Meeting of the Satellite Division, Fort Worth, TX - 25-28 September 2007*, 2007.

[76] F. van Graas A. Alaqeeli, J. Starzyk. Real-time acquisition and tracking for gps receivers. 2003.

[77] NavSAS. Website: http://www.navsas.eu.

[78] V.F. Kroupa. *Phase Lock Loops and frequency synthesis*. Wiley, 2003.

[79] M. Fantino L. Lo Presti, M. Pini. *Digital signal processing in GNSS receivers*. Wiley, 2011.

[80] L. Lo Presti-M. Fantino E. Falletti, M. Pini. High dynamics and false lock resistant gnss carrier tracking loops. *International Technical Meeting of the Satellite Division, Fort Worth, TX - 25-28 September*, 2007.

[81] B. Motella E. Falletti, D. Margaria. Educational library of gnss signals for navigation. *Coordinates Issue 8, Vol.V, pp.30-34, ISSN: 0973-2136, August*, 2009.

[82] Chen Chen. Detection of ionospheric spatial gradients, 2010.

[83] K. G. Budden. *The propagation of radio waves: the theory of radio waves of low power in the ionosphere and magnetosphere*. Cambridge: Cambridge University Press, 1988.

[84] S. Chapman. The absorption and dissociative or ionizing effect of monochromatic radiation in an atmosphere on a rotating earth. *Proceedings of the Physical Society Volume 43 Number 1*, 1931.

[85] Q. Zhoul F. van Graas W. Pelgrum J. Wangl, Y. Morton. Time-frequency analysis of ionosphere scintillations observed by a gnss receiver array. 2012.

[86] M. Abdullah M. Ismail N. Yaacob, M. H. Jusoh. Monitoring the tec variation using gps dual frequency system during quiet and disturbed day.

[87] U. J. Lindqwister X. Pi L. Sparks B. D. Wilson A. J. Mannucci, B. A. Iijima. Gps and ionosphere. *Revised Submission to URSI Reviews of Radio Science, March 1999 edition*, 1999.

[88] A. Coster W. Rideout. Automated processing for global total electron content data. *GPS solution*, 2006.

[89] P. Chandrasekaran F. van Graas N. Matteo, Y. Morton. Higher order ionosphere errors at arecibo, millstone, and jicamarca. *Proceedings of the 22nd International Technical Meeting of The Satellite Division of the Institute of Navigation (ION GNSS 2009), Savannah, GA, pp. 2739-2740, September 2009*, 2009.

[90] van Graas F. Morton Y. T., Zhou Q. Assessment of second-order ionosphere error in gps range observables using arecibo incoherent scatter radar measurements. *Radio Science, Vol. 44, January 2009*, 2009.

[91] J. A. Klobuchar. Ionospheric time-delay algorithm for singlefrequency gps users. *Aerospace and Electronic Systems, IEEE Transactions, May 1987, pp. 325-331*, 1987.

[92] B. Nava S. M. Radicella. Nequick model: origin and evolution.

[93] T. A. Skidmore D. C. Bruckner, F. van Graas. Algorithm and flight test results to exchange code noise and multipath for biases in dual frequency differential gps for precision approach. *Navigation, vol. 57, No. 3, pp. 213-229, Fall 2010*, 2010.

[94] CODE. Website: http://www.aiub.unibe.ch/download.

[95] CODE. Website: ftp://fto.unibe.ch/aiub/BSWUSER50/TXT/AIUB_AFTP.README.

[96] S. Schaer. Overview of gnss biases. *Workshop on GNSS Biases, Uni Bern, 18-19 January 2012, Swiss Federal Office of Topography*, 2012.

[97] CRS manual. Website: http://www.cfrsi.com/pdf/NewREceiverBrochure_GPSWorl_final.pdf.

[98] N. S. Chung I. S. Chang E. Kawai F. Takahashi C. B. Lee, D. D. Lee. Development of a gps codeless receiver for ionospheric calibration and time transfer. *IEEE TRANSACTIONS ON INSTRUMENTATION AND MEASUREMENT, VOL. 42, NO. 2, APRIL 1993*, 1993.

[99] R. B. Langleyb J. W. MacDougallc M. J. Nicollsd D. R. Themensa, P.T. Jayachandrana. Determining receiver biases in gps-derived total electron content in the auroral oval and polar cap region using ionosonde measurements. *General Assembly and Scientific Symposium, 2011 XXXth URSI, 13-20 Aug. 2011*, 2011.

[100] JPL. Website: http://igscb.jpl.nasa.gov/.

[101] J. Thompson S. Gonzalez J. J. Sojka V. Eccles, H. Vo. Database of electron density profiles from arecibo radar observatory for the assessment of ionospheric models. *Space Weather, 9*, 2011.

[102] W.E. Gordon. Incoherent scattering of radio waves by free electrons with applications to space exploration by radar. *Proceedings of the IRE*, Volume: 46, Issue: 11 Page(s): 1824 - 1829, 1958.

[103] M. Milla E.Kudeki. *Incoherent Scatter Radar - Spectral Signal Model and Ionospheric Applications, Doppler Radar Observations - Weather Radar, Wind Profiler, Ionospheric Radar, and Other Advanced Applications*. American Institute of Aeronautics and Astronautics, Inc., 2012.

[104] G. Wannberg. Incoherent scatter radar techniques: an overview, 2005.

[105] G. Galati. *Radar e navigazione*. Texmat, 2004.

[106] A. Haug O. Bratteng. Model ionosphere at high latitude, eiscat feasibility study. *Report. No. 9. The Auroral Observatory, TromsÃ¶ Ju1y 1971*, 1971.

[107] M. P. Sulzer. Website: www.naic.edu/~isradar/is/intro/wdexp.pdf.

[108] E. Yizengaw J. Le Marshall C.-S. Wang B. A. Carter D. Wen K. Zhang R. J. Norman, P. L. Dyson. Radio occultation measurements from the australian microsatellite fedsat. *IEEE TRANSACTIONS ON GEOSCIENCE AND REMOTE SENSING, VOL. 50, NO. 11, NOVEMBER 2012*, 2012.

[109] F. van Graas S. Gunawardena. High fidelity chip shape analysis of gnss signals using a wideband software receiver. *Proceedings of the 25th International Technical Meeting of The Satellite Division of the Institute of Navigation (ION GNSS 2012), Nashville, TN, September 2012*, 2012.

[110] F. van Graas S. Gunawardena. Analysis of gps pseudorange and natural biases using a software receiver. *Proceedings of the 25th International Technical Meeting of The Satellite Division of the Institute of Navigation (ION GNSS 2012), Nashville, TN, September 2012n*, 2012.

[111] A. MacAulay A. J. van Dierendonck S. Shanmugam, J. Jones. Evolution to modernized gnss ionospheric scintillation and tec monitoring. *IEEE/ION PLANS 2012, April 24-26, Myrtle Beach, SC*, 2012.

Publications

(I) F. van Graas, S. Craig, W. Pelgrum, S. Ugazio, Laboratory and Flight Test Analysis of Rubidium Frequency Reference Performance, accepted on January 9th, 2013, and to be published on Navigation, Journal of the Institute of Navigation, Summer Issue 2013.

(II) S. Ugazio, M. Fantino, L. Lo Presti, Design of Second and Third Order PLLs with Adaptive Bandwidth in Real Time, Proceedings of the 2011 International Technical Meeting of The Institute of Navigation, San Diego, CA, January 2011, pp. 1281-1292.

(III) S. Ugazio, L. Lo Presti, M. Fantino, Design of real time adaptive DPLLs for generic and variable Doppler frequency, Localization and GNSS (ICL-GNSS), 2011 International Conference on , vol., no., pp.169-174, 29-30 June 2011

(IV) S. Ugazio, F. van Graas, W. Pelgrum, Total Electron Content measurements with uncertainty estimate, Satellite Navigation Technologies and European Workshop on GNSS Signals and Signal Processing, (NAVITEC), 2012 6th ESA Workshop on , vol., no., pp.1-8, 5-7 Dec. 2012

(V) M. Pini, M. Fantino, A. Cavaleri, S. Ugazio, L. Lo Presti, Signal Quality Monitoring Applied to Spoofing Detection, Proceedings of the 24th International Technical Meeting of The Satellite Division of the Institute of Navigation (ION GNSS 2011), Portland, OR, September 2011, pp. 1888-1896.